

Relevance of spatial quenched disorder in the Diffusive Epidemic Process

Valentin Anfray* and Hong-Yan Shih†

*Institute of Physics, Academia Sinica. No. 128, Sec. 2,
Academia Rd., Nangang Dist., Taipei City 115201, Taiwan (R.O.C.).*

The diffusive epidemic process is an example of reaction-diffusion system where diffusion constants of healthy and infected particles determine the universality class of the absorbing phase transition. Introducing spatial quenched disorder in the contamination rates and the diffusion rates of each species leads to a rich phase diagram depending on the disorder distribution. Particularly, signature of different infinite disorder fixed points and lack of active phase are reported. The relevance of disorder is correctly predicted by the Harris criterion in light of the effective macroscopic diffusion rates. However, the effective disorder strength depends on which diffusion rate heterogeneities are introduced.

Intrinsic heterogeneity, or quenched disorder, is ubiquitous in the real world, and plays a significant role in many notable phenomena such as localization [1], spin glass [2] and ecological patterns [3]. Quenched disorder can drastically impact the critical properties of phase transitions in both equilibrium and non-equilibrium systems. In the directed percolation universality class [4–7], which governs absorbing state phase transitions in various systems such as contact process for epidemic spreading, quenched disorder is relevant and leads to a non-conventional fixed point [8–12].

The diffusive epidemic process (DEP) [13, 14] is another paradigm model for epidemic spreading [15–17], where two types of particles—healthy (A) and infected (B)—diffuse with rates D_A and D_B respectively, and undergo onsite reactions upon contact ($A+B \rightarrow 2B$) at rate λ with spontaneous recovery ($B \rightarrow A$) at rate $1/\tau$, thus conserving total particle number. Remarkably, DEP with positive diffusion rates exhibits absorbing phase transitions to a state with only A , which belong to three distinct universality classes based on the relative values of the diffusion rates [18]. In the two cases where $D_A = D_B$ and $D_B > D_A$, the field theory [13, 14] and the numerical simulations show distinct critical behavior at $D \leq 2$ [19–23]. For $D_A > D_B$, analytical predictions suggested a discontinuous transition [14], whereas numerical simulations revealed a continuous phase transition [19–23]. Besides the fundamental interest of its statistical properties, DEP serves as a simplified model with positive feedback for pattern formation such as cell polarization [24, 25].

While heterogeneities naturally arise at various scales from populations to individual cells, the impact of intrinsic inhomogeneities on DEP has not been extensively studied. Mechanisms such as the cytoskeleton [26, 27], scaffold proteins [28], and ion channels [29] create spatial heterogeneities within cells, and how to understand the effects of impurities in minimal models such as DEP remains an important area for further investigation.

The explicit dependence on diffusion rates in the phase transition behavior in DEP raises a question regarding spatial quenched disorders: can the behavior where local rates are influenced by spatial quenched disorder be understood in the light of its effective global homogeneous rates? Predictions regarding the effects of heterogeneities are often made using scaling arguments [31], such as the Harris criterion [32]. This criterion relates the stability of a clean critical point against weak uncorrelated spatial disorder to the correlation length exponent ν_\perp through the inequality $d\nu_\perp > 2$ where d represents the system’s dimensionality. When this criterion is violated, the critical behavior changes. For directed percolation, it leads to an exotic fixed point referred to as Infinite Disorder Fixed Point (IDFP) [8–12], due to the divergence of the effective disorder strength under coarse graining. Such a fixed point is characterized by an activated dynamical scaling [33]. At its vicinity, power-law Griffith singularities [34] emerge due to slow decay of rare-regions being in the opposite phase [35]. For the one-dimensional DEP, Harris criterion predicts that disorder is relevant for $D_A > D_B$ where $\nu_\perp < 2$ [21] and marginal for $D_A \leq D_B$ where $\nu_\perp = 2$ [14] [36]. However, in cases with heterogeneous diffusion rates where some local regions may have $D_A > D_B$ while others $D_A \leq D_B$, it is unclear which ν_\perp should be used to predict the relevance of disorder.

The purpose of this paper is to explore numerically the effect of spatial quenched disorder on the DEP paradigm of absorbing phase transition and show that a rich phase diagram emerges from nontrivial interplay between heterogeneity-driven activity fluctuations induced by reactions and motility. We demonstrate that the critical properties in general cannot be solely understood through the global effective rates as disorder can lead to new fixed points. In our work, we study the activity spreading behavior [7, 37] through extensive numerical simulations using a Gillespie-type algorithm [38], enhanced by a novel approach that simulates infinite system sizes, reducing finite-size effects and improving computational efficiency. We begin by investigating the relevance of disorder with spatially dependent contamination rates, and find numerical evidence that supports predictions from the Harris criterion. Specifically, contamination rate disorder is relevant for $D_A > D_B$ and leads to a

* valentin.anfray@gmail.com

† hongyan@as.edu.tw

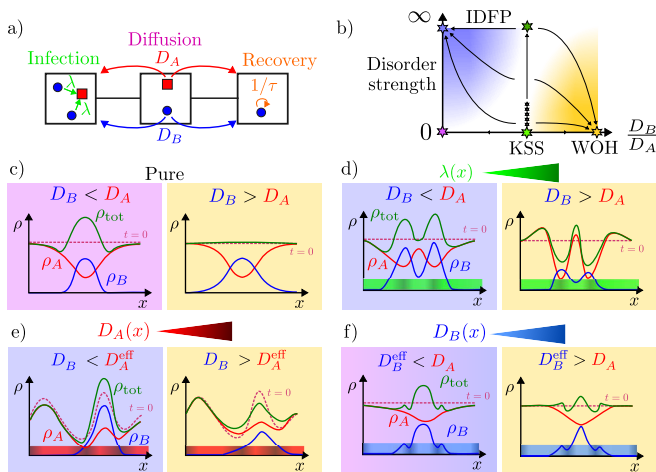


FIG. 1. (a) Schematic of the Diffusive Epidemic Process. A (red) and B (blue) particles diffuse with rates D_A and D_B , respectively. B particles infect A at rate λ and recover at rate $1/\tau$. (b) Schematic of the Renormalization Group flow depending on the disorder strength and the ratio D_B/D_A for $D_A, D_B > 0$. The three pure fixed points are indicated in pink ($D_A > D_B$), green ($D_A = D_B$) [13] and yellow ($D_A < D_B$) [14]. When $D_B < D_A$, disorder leads to an infinite disorder fixed point (IDFP), in blue. For $D_A = D_B$, critical properties depends on the initial disorder strength with slowly varying exponents up to another IDFP. (c-f) Density profiles of A (red), B (blue), and total density $A + B$ (green) at time $t > 0$, starting from a A population with a single infected seed (dotted line). Background colors indicate critical behaviors showed in (b). (c) Even in the pure case, the ratio D_B/D_A strongly affects spreading: for $D_B < D_A$, subdiffusive behavior emerges and $\nu_{\perp} < 2$ [21], while for $D_B > D_A$, spreading is superdiffusive and $\nu_{\perp} \approx 2$ [30]. (d) Disorder in λ : When $D_B > D_A$, the system dynamics tend to mitigate disorder effects by lowering the total density where λ is large, making it irrelevant. Conversely, for $D_B < D_A$, B particles more strongly localize, leading to an IDFP. (e) Disorder in the diffusion rate D_A . Similar to (d), with density differences between high- and low-diffusion regions being smoothed out ($D_B > D_A^{\text{eff}}$) or enhanced ($D_B < D_A^{\text{eff}}$). (f) Disorder in D_B : results remain ambiguous, as the dynamics closely resemble those of the pure system. This suggests that the disorder effect is weaker and challenging to analyze numerically.

new IDFP with evidences of Griffith singularities in the subcritical regime. Second, we introduce heterogeneities in the diffusion rates and demonstrate that the effective global diffusion rate can be used to predict the relevance of disorder. However, strong initial disorder can escape this prediction and may even suppress the active phase. Lastly, we consider local correlation between the diffusion rates D_A and D_B , to model time-independent spatial density variations, and establish a link with the disordered contact process dynamics to have a better understanding on the critical properties.

The fate of activity spreading can be physically understood through the interacting dynamics, as shown in Fig. 1c-f). In the pure case, activity spreading is

strongly affected by the ratio of diffusion rates. For $D_B < D_A$, A spreads quickly and leaves slow B clusters surrounded by a local depletion region, leading to subdiffusive spreading of B clusters (see Fig. 1c)) and [21]. On the other hand, superdiffusion in B is observed in the case of $D_B > D_A$ (Fig. 1c)). Introducing heterogeneities in the λ rates facilitates infection in specific regions. When $D_B > D_A$, such regions tend to be less populated (see Fig. 1d)) as infected particles spread faster. Consequently, the dynamics mitigate the effect of disorder, providing a physical interpretation for its irrelevance. Conversely, when $D_B < D_A$, regions with higher infection rates become more populated. Compared to the pure case, this typically amplifies the density differences between regions and localize the position of dense infected areas. As a result, disorder affects the spreading behavior differently than in the pure case, suggesting its relevance. A similar reasoning applies to heterogeneous D_A rates, where regions with a higher particle density (low D_A) are more susceptible to infection (see Fig. 1e)). For heterogeneities in D_B (see Fig. 1f)), the situation is more complex, as it is difficult to predict whether an infection will persist longer in regions with high or low D_B . Moreover, individual sites alone with large or low D_B are not expected to alter significantly the dynamics. Instead, a subdiffusive cluster or a superdiffusive spreading process must extend over a sufficiently large region. Consequently, we expect the disorder strength to be weaker, making it more challenging to study numerically due to larger transient.

Observables of interest—Key quantities for studying the activity spreading are [7, 37, 39]: survival probability $P_s(t)$, total number of B particles $N_B(t)$, and mean-square displacement $R^2(t)$ of B particles averaged only over surviving samples. In the thermodynamic limit, these quantities are expected to follow the scaling forms:

$$\begin{aligned} P_s(\Delta, t) &= b^{\beta'/\nu_{\perp}} \tilde{P}_s(\Delta b^{-1/\nu_{\perp}}, tb^z), \\ N_B(\Delta, t) &= b^{\Theta z} \tilde{N}_B(\Delta b^{-1/\nu_{\perp}}, tb^z), \\ R^2(\Delta, t) &= b^{-2} \tilde{R}^2(\Delta b^{-1/\nu_{\perp}}, tb^z), \end{aligned}$$

where Δ is the distance from the critical point, b is an arbitrary scaling factor, and $z = \nu_{\parallel}/\nu_{\perp}$ is the dynamical exponent. The exponent $\Theta = d/z - \alpha - \delta$ is the so-called slip exponent, where $\alpha = \beta/\nu_{\parallel}$ and $\delta = \beta'/\nu_{\parallel}$. In general, $\alpha \neq \delta$, except when the system exhibits rapidity-reversal symmetry [7]. At criticality, these quantities asymptotically obey power-law behaviours of the form [40]:

$$P_s(t) \sim t^{-\delta}, \quad N_B(t) \sim t^{\Theta}, \quad R_s^2(t) \sim t^{2/z}. \quad (1)$$

To estimate the critical contamination rate and the critical exponents, we study the time dependence of effective exponents [41–43].

A challenge in simulating DEP is tracking the time evolution of the entire configuration to ensure particle conservation. To overcome this, we develop a new numerical algorithm [30] that updates only a local region of

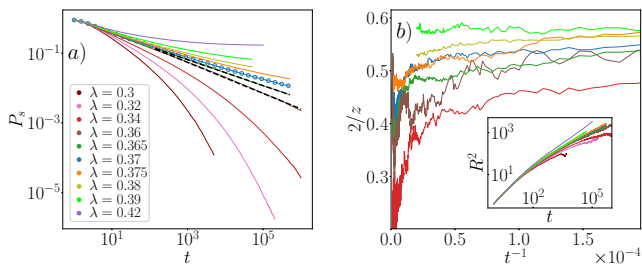


FIG. 2. λ -disorder with $1 = D_A > D_B = 0.375$, $p_\lambda = 0.3$, $c = 0.2$. a) Evolution of the surviving probability P_s in a log-log scale. Power-law decay of P_s are found (black dotted-line) outside of the estimated critical point (circle, blue line) and not at it. b) Evolution of the effective dynamical exponent $2/z$ decays to abnormally low values. It corresponds to a slower than a power-law growth of the mean-squared displacement R^2 (inset).

the system, effectively simulating an infinite system from the perspective of the infected particles up to a specified maximum time T_{\max} . Our estimations of the critical exponents in the pure cases align with the most recent numerical simulations [30].

Disorder in the contamination rates—We start by introducing heterogeneities in the contamination rate (referred as λ -disorder) that only induces fluctuation in the position of the critical point. Hence, the Harris criterion is expected to hold and predicts a relevance of the disorder only when $D_A > D_B$. We choose a binary probability distribution for λ at site i [8, 44]

$$P(\lambda_i) = (1 - p_\lambda)\delta(\lambda_i - \lambda) + p_\lambda\delta(\lambda_i - c\lambda), \quad (2)$$

where c controls the strength of the impurities and p_λ is their probability, both with values between 0 and 1.

We focus on the case $D_A > D_B$, which holds greater biological significance [24, 25] and study the evolution of the survival probability $P_s(t)$ (Fig. 2a). Unlike the typical critical behavior, at the estimated critical point (circle) [30] the decay of $P_s(t)$ is no longer a power law, while for smaller contamination rates, $P_s(t)$ shows power-law decay up to the maximum time considered (black dotted lines). Similarly, the mean-square displacement also falls off a power law with a significantly declining exponent at large times, corresponding to an unusually large dynamical exponent $z(t)$ that indicates especially slow dynamics. These observations are not compatible with a conventional fixed point but can be well-explained by an infinite-disorder fixed point (IDFP) [31, 33, 45], surrounded by Griffith phases with power-law singularities, that features activated scaling forms [46, 47]:

$$P_s(t) \sim [\ln(t/t_0)]^{-\bar{\delta}}, \quad N_B(t) \sim [\ln(t/t_0)]^{\bar{\Theta}}, \\ R^2(t) \sim [\ln(t/t_0)]^{2/\psi}, \quad (3)$$

where the tunneling exponent ψ and the non-universal microscopic time scale t_0 relate correlation lengths ξ_\perp and ξ_\parallel by $\ln(\xi_\parallel/t_0) \sim \xi_\perp^\psi$. Investigating the sign of the

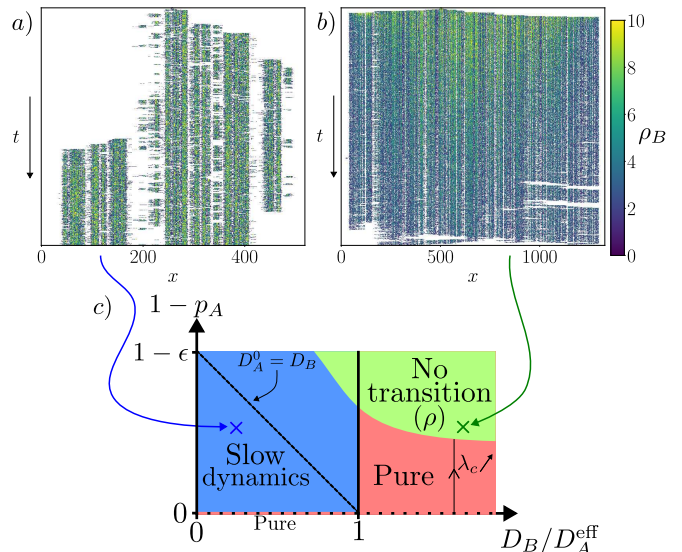


FIG. 3. D_A -disorder with large D_A^1 fixed ($= 2000$). (a) Time evolution (kymograph) starting from a seed with parameters $1.4 = D_A^0 > D_B$, $p_A = 0.5$, at the estimated critical point $\lambda_c = 0.22$. Infection can survive for a long time in large, densely populated regions formed by neighboring sites with $D_{A,i} = D_A^0$. The spreading speed is limited by the time required for the infection to reach the next dense region, which is separated by low-density areas. (b) Same as (a) with $0.1 = D_A^0 < D_B$ and a high contamination rate $\lambda = 50$. Initially, the infection spreads rapidly but eventually stops due to the presence of large regions with low particle density, which take longer to be overcome. This delay allows the system to equilibrate according to the diffusion rates D_B and D_A^0 , leading to a reduction in particle density per infected site since $D_A^0 < D_B$. When this density becomes too low, spontaneous site recovery can occur independently of λ , leading to the absence of an active phase. (c) Schematic phase diagram depending on $1 - p_A$ the probability to have sites with D_A^1 which can represent the strength of the initial spatial heterogeneities in the system. It stops at $p_A = \epsilon > 0$ as $p_A = 0$ corresponds to the pure case with $D_A^1 > D_B$. When $D_A^{\text{eff}} < D_B$ (red region), the system exhibits critical properties consistent with the pure case, and the critical threshold λ_c increases as p_A decreases. Eventually, λ_c diverges, indicating a lack of transition (green region). The position of the boundaries depends on the total density ρ . In the slow region, the dynamical exponent $2/z$ is lower than in the pure case. Numerical simulations suggest that the critical behavior is governed by an Infinite Disorder Fixed Point (IDFP).

exponents [30], we find this IDFP to be different from the IDFP of the disordered contact process.

We leave in [30] the study of the cases: $D_B > D_A$ and $D_A = D_B$. In the former case, we found that the critical properties align with pure ones, confirming marginal irrelevance of disorder. The second is more puzzling as our results suggest a weak universality scenario, with static exponents (β, ν_\perp) unaffected and z dependent on the disorder strength.

Disorder in the diffusion rates—Given that the diffusion rates $D_{A,i}$ affect the mean number of particles per

site in absence of infection, introducing heterogeneities in the diffusion rates is effectively studying how the spreading is affected by an heterogeneous initial density that is not only due to stochastic fluctuations. We consider a binary distribution for diffusion rates at site i :

$$\mathcal{P}(D_{X,i}) = p_X \delta(D_{X,i} - D_X^0) + (1 - p_X) \delta(D_{X,i} - D_X^1), \quad (4)$$

where $X = A, B$. By convention, $D_X^1 > D_X^0 > 0$, classifying sites with D_X^0 as slow and those with D_X^1 as fast. The parameter p_X represents the probability of a site being slow. From this, the effective diffusion rate is given by $1/D_X^{\text{eff}} = p_X/D_X^0 + (1 - p_X)/D_X^1$, corresponding to the long-time diffusion rate of a particle diffusing without interactions in a 1D system. We use D_A^{eff} and D_B^{eff} to predict critical properties as if no disorder were present.

We focus on a notable case where only the diffusion rates of healthy A particles are heterogeneous (drawn from Eq. 4), while $D_{B,i} = D_B$. Depending on D_A^0, D_A^1, p_A , a theoretically rich phase diagram emerges, as illustrated in Figure 3c) for $D_A^1 \gg 1$, similar conclusions still hold for finite D_A^1 [30]. In particular, a slow dynamics and an absence of transition are observed. Slow dynamics refer to a dynamical exponent z exceeding that of the pure system, which may indicate an IDFP where z is formally infinite. We leave in [30] the numerical evidences and focus here only on two specific examples to illustrate the new dynamics emerging. In Figure 3a), infected regions are strongly localized on regions where the sites have a low diffusion rate $D_{A,i} = D_A^0$, i.e., where the density of A particles is expected to be the largest. Because $D_B < D_A^0$, density of newly infected regions increases which further increase their surviving time. The spread is restricted by the time it takes for the infection to cross sparse regions and reach the next region of high density. This new behaviour leads to a slower dynamics. And critical properties are compatible with an IDFP scenario. In Figure 3b), the infection starting from a seed spreads quickly due to the large contamination rate ($\lambda = 50$), until it reaches large regions with a low particle density. These regions require more time for the infected particles to traverse, as they recover before being able to infect new particles. During that period, the average number of particles per site slowly converges to an equilibrium value. Since $D_B > D_A^0$, the number of particles in the infected region decreases until flux conservation is reached, given by $\rho_A D_A^0 = \rho_B D_B$. If D_A^0 is sufficiently low compared to D_B , infected sites can recover even at high contamination rates, leading to the absence of an active state at late times and, consequently, the absence of a phase transition.

In [30], a simple model is used to derive the fastest spread of the infection, providing an upper bound for the exponent $2/z$. We show that it explicitly depends on the disorder distribution implying that disorder can lead to critical properties different from those of the pure system, in agreement with the phase diagram in Fig. 3c).

In the reverse case of D_B -disorder, where only $D_{B,i}$ is heterogeneous, the critical properties resemble those

of the pure system for both $D_B^{\text{eff}} < D_A$ or $D_B^{\text{eff}} > D_A$ [30]. Surprisingly, no sign of an IDFP is found. Usually, the slow dynamics around an IDFP is well understood by the concept of rare regions devoid of any defect which are locally in the active phase [48]. For D_B -disorder, we expect such regions to be defined over a mesoscopic characteristic length scale as discussed in [30]. Hence, the lack of numerical evidence of a relevance of the disorder when $D_B^{\text{eff}} < D_A$ may result from an effective weaker effect of D_B -disorder, which would require significantly longer simulation times to converge to the disordered fixed point.

Correlated diffusion disorder—We consider perfectly correlated on-site diffusion rates, given by $D_{A,i} = \mu D_{B,i} = \mu D_i$ with $\mu > 0$. In particular, we focus on the case $\mu = 1$, which corresponds to a time-independent (on average) spatially varied density profile, a more suitable scenario for studying epidemics in human populations. We use again the binary distribution in Eq. 4 with p the probability to have a site i with $D_i = D^0$ and otherwise D^1 so that $D_{A,i} = D_{B,i} = D_i$. To predict the effect of disorder, we consider the following assumption: the dynamics is governed by the dense regions. Then, by coarse graining the microscopic dynamics and considering a dense region to be active or inactive if there are infected particles or not. We arrive to a contact process like model where the effective contamination rate depends on the distance between the dense regions, as illustrated in Fig. 4a). From this simple picture, if the slow sites (dense regions) are equally spaced, then the critical properties should belong to the pure DP universality class and otherwise to the disordered one. A periodic quenched disorder is not expected to change the critical properties, but can affect its intermediate dynamics as shown in Fig. 4b). As D^0 is lowered, an initial plateau of $R^2(t)$ emerges whose end is related to a new mesoscopic time scale corresponding to the infection time between neighboring dense regions. When such time scale, which depends on the disorder distribution, is larger compared to the other microscopic time scales, we expect our simple picture to qualitatively hold. The growth of R^2 after this plateau is faster than expected and can even be compatible with $2/z_{\text{DP}}$, with z_{DP} the dynamical exponent of the DP universality class, depending on the disorder distribution.

Randomly spacing the slow sites changes dramatically the dynamics. The growth of R^2 is much slower (dash-dotted green line) and is compatible with an activated scaling. Such critical behaviour is also observed in the disordered contact process [46, 47] but our data cannot conclude about the possibility of being controlled by the same IDFP. Moreover, the survival probability P_s with a random disorder decays differently in the absorbing phase than with a periodic disorder as shown in Fig. 4c). The decay is not a clear power-law up to the maximum time considered, hence the existence of an extended Griffith phase is still unknown. This simple picture provides insight into how disorder strength can alter critical prop-

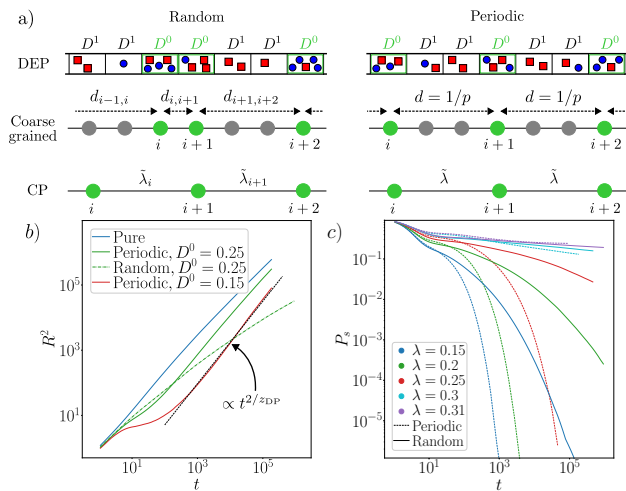


FIG. 4. a) Schematic picture of the perfectly correlated diffusion disorder $D_{A,i} = D_{B,i} = D^{0/1}$ where the disordered sites with D^0 are randomly inserted (left) with probability p or periodically spaced. Below, a coarse grained picture where only the information relative to the sites with D^0 , infected/non-infected and the distance to the neighbours $d_{i,j}$, are kept. It finally corresponds to the contact process with random contamination rate $\tilde{\lambda}_i$ (left) or with the same $\tilde{\lambda}$ (right). b) Mean square displacement R^2 at the critical point for different D^0 with $p = 0.1, D^1 = 1$. Depending on the disorder distribution, the intermediate growth of R^2 can be compatible with the DP dynamical exponent (red curve). Randomizing the position of the sites with D^0 leads to a much slower growth (dotted green line). c) Survival probability P_s with t for a periodic (dotted) and random (plain) disorder with identical $D^0 = 0.25, D^1 = 1, p = 0.1$. The different decay of the survival time in the absorbing phase for random disorder is attributed to the slow recovery of active rare regions formed by adjacent sites with D^0 .

erties when weak disorder is marginal ($D_A = D_B$) and allows predicting its impact based on the disordered contact process.

Discussion.—We have shown that the effect of quenched spatial disorder on the one-dimensional DEP leads to a variety of new behaviors depending on the relative value of effective macroscopic diffusion rates. New infinite disorder fixed points are identified both in the cases with disorder in the contamination rate and diffusion rate of healthy particles, accompanied by Griffith phases with power-law scaling outside the critical regime.

In cell polarity, this feature may imply that spontaneous patterns can be observed for an extended amount of time due to slow dynamics, which may facilitate further biological response such as budding. The recruitment rate of molecules on the cellular membrane—analogue to the contamination rate in DEP—can be affected by pheromones [49], and the non-uniform protein distribution inside single cells can be related to spatial dependence of diffusion rates [27, 50–52]. These open possible experimental observations for the disorder effect in DEP. Relevance of disorder by the Harris criterion is well predicted by the mean of effective diffusion rates. However, strongly spatially heterogeneous system can still lead to new behavior as even suppressing the transition itself. Lack of numerical evidence of a relevance of D_B disorder is expected to be due to an effective weaker disorder that remains to be verified in the future.

To model epidemics in which populations at specific locations remain unchanged while exhibiting strong spatial variations at different scale [53–57], we have also considered on-site correlated diffusion rates between the infected and healthy individuals. Strong enough spatial density variations are shown to be relevant perturbations leading to an infinite disorder fixed point. While the emergence of slow dynamics due to disorder in epidemic models is already well-documented, particularly in studies of the SIS/contact process [8–12], role of spatial density variation was absent.

A promising direction for future research is to deepen our understanding when disorder in diffusion rates becomes relevant, and exploring the possibility of studying the genuine IDFP identified here using strong-disorder renormalization group techniques. Additionally, extending this work to higher-dimensional systems and networks to verify if those finding still hold would be valuable to get closer to realistic systems. It would also allow to compare with the effect of connectivity disorder that has been found to be irrelevant at $d = 2$ [23].

We gratefully acknowledge valuable discussions with Frédéric van Wijland. This work was supported by grants from the National Science and Technology Council, Taiwan (Grant No. NSTC 109-2112-M-001-017-MY3 and 111-2112-M-001-027-MY3) and Academia Sinica Career Development Award (Project No. AS-CDA-114-M02). VA acknowledges support from Academia Sinica Postdoctoral Scholar Program.

[1] P. W. Anderson, Absence of Diffusion in Certain Random Lattices, *Phys. Rev.* **109**, 1492 (1958).
 [2] M. Mezard, G. Parisi, and M. A. Virasoro, *Spin glass theory and beyond* (World Scientific, 2004).
 [3] S. T. A. Pickett and M. L. Cadenasso, Landscape Ecology: Spatial Heterogeneity in Ecological Systems, *Sci* **269**, 331 (1995).

[4] P. Grassberger, On phase transitions in Schlögl’s second model, *Z. Phys. B Condens. Matter* **47**, 365 (1982).
 [5] H. K. Janssen, On the nonequilibrium phase transition in reaction-diffusion systems with an absorbing stationary state, *Z. Phys. B Condens. Matter* **42**, 151 (1981).
 [6] E. Domany and W. Kinzel, Equivalence of Cellular Automata to Ising Models and Directed Percolation,

- Phys. Rev. Lett. **53**, 311 (1984).
- [7] M. Henkel, *Non-equilibrium phase transitions* (Springer, 2008).
- [8] J. Hooyberghs, F. Iglói, and C. Vanderzande, Absorbing state phase transitions with quenched disorder, Phys. Rev. E **69**, 066140 (2004).
- [9] T. Vojta, A. Farquhar, and J. Mast, Infinite-randomness critical point in the two-dimensional disordered contact process, Phys. Rev. E **79**, 011111 (2009).
- [10] T. Vojta, Monte Carlo simulations of the clean and disordered contact process in three dimensions, Phys. Rev. E **86**, 051137 (2012).
- [11] C. Buono, F. Vazquez, P. A. Macri, and L. A. Braunstein, Slow epidemic extinction in populations with heterogeneous infection rates, Phys. Rev. E **88**, 022813 (2013).
- [12] R. Juhász, G. Ódor, C. Castellano, and M. A. Muñoz, Rare-region effects in the contact process on networks, Phys. Rev. E **85**, 066125 (2012).
- [13] R. Kree, B. Schaub, and B. Schmittmann, Effects of pollution on critical population dynamics, Phys. Rev. A **39**, 2214 (1989).
- [14] F. van Wijland, K. Oerding, and H. J. Hilhorst, Wilson renormalization of a reaction–diffusion process, Physica A **251**, 179 (1998).
- [15] M. Slattery, Ecology, Genetics, and Evolution of Metapopulations Edited by I. Hanski and O. E. Gaggiotti (University of Helsinki). Elsevier Academic Press, Amsterdam. 2004. xix + 696 pp. 17 × 25 cm. \$54.95. ISBN 0-12-323448-4., J. Nat. Prod. **67**, 2156 (2004).
- [16] V. Colizza, R. Pastor-Satorras, and A. Vespignani, Reaction–diffusion processes and metapopulation models in heterogeneous networks, Nat. Phys. **3**, 276 (2007).
- [17] V. Colizza and A. Vespignani, Epidemic modeling in metapopulation systems with heterogeneous coupling pattern: Theory and simulations, J. Theor. Biol. **251**, 450 (2008).
- [18] The case $D_A = 0$ featuring infinitely many absorbing states and belonging to the Manna universality class [?] is not discussed here.
- [19] D. S. Maia and R. Dickman, Diffusive epidemic process: theory and simulation, J. Phys. Condens. Matter **19**, 065143 (2007).
- [20] A. M. Filho, G. Corso, M. L. Lyra, and U. L. Fulco, Critical properties of the diffusive epidemic process obtained via an automatic search technique, J. Stat. Mech: Theory Exp. **2010**, P04027 (2010).
- [21] B. Polovnikov, P. Wilke, and E. Frey, Subdiffusive Activity Spreading in the Diffusive Epidemic Process, Phys. Rev. Lett. **128**, 078302 (2022).
- [22] R. Dickman and D. S. Maia, The nature of the absorbing-state phase transition in the diffusive epidemic process, J. Phys. Math. Theor. **41**, 405002 (2008).
- [23] D. S. M. Alencar, T. F. A. Alves, G. A. Alves, F. W. S. Lima, A. Macedo-Filho, and R. S. Ferreira, Two-dimensional diffusive epidemic process in the presence of quasiperiodic and quenched disorder, J. Stat. Mech: Theory Exp. **2023**, 043205 (2023).
- [24] S. J. Altschuler, S. B. Angenent, Y. Wang, and L. F. Wu, On the spontaneous emergence of cell polarity, Nat **454**, 886 (2008).
- [25] F. Brauns, J. Halatek, and E. Frey, Phase-Space Geometry of Mass-Conserving Reaction-Diffusion Dynamics, Phys. Rev. X **10**, 041036 (2020).
- [26] T. Hohmann and F. Dehghani, The Cytoskeleton—A Complex Interacting Meshwork, Cells **8**, 362 (2019).
- [27] L. Xiang, K. Chen, R. Yan, W. Li, and K. Xu, Single-molecule displacement mapping unveils nanoscale heterogeneities in intracellular diffusivity, Nat. Methods **17**, 524 (2020).
- [28] M. C. Good, J. G. Zalatan, and W. A. Lim, Scaffold Proteins: Hubs for Controlling the Flow of Cellular Information, Sci **332**, 680 (2011).
- [29] D. C. Gadsby, Ion channels versus ion pumps: the principal difference, in principle, Nat. Rev. Mol. Cell Bio. **10**, 344 (2009).
- [30] See Supplemental Material at URL-will-be-inserted-by-publisher for numerical details, estimations of critical contamination rates and critical exponents, complementary figures, movie descriptions.
- [31] F. Iglói and C. Monthus, Strong disorder RG approach of random systems, Phys. Rep. **412**, 277 (2005).
- [32] A. B. Harris, Effect of random defects on the critical behaviour of Ising models, J. Phys. C Solid State Phys. **7**, 1671 (1974).
- [33] D. S. Fisher, Critical behavior of random transverse-field Ising spin chains, Phys. Rev. B **51**, 6411 (1995).
- [34] R. B. Griffiths, Nonanalytic Behavior Above the Critical Point in a Random Ising Ferromagnet, Phys. Rev. Lett. **23**, 17 (1969).
- [35] T. Vojta and J. A. Hoyos, Criticality and Quenched Disorder: Harris Criterion Versus Rare Regions, Phys. Rev. Lett. **112**, 075702 (2014).
- [36] There is still no consensus in between the numerical simulations and with the field-theoretic analysis. For the purpose of this study, this is particularly important for the case $D_A > D_B$ where a discontinuous transition is predicted but not supported by all the recent numerical simulations. More details can be found in [30].
- [37] P. Grassberger and A. de la Torre, Reggeon field theory (Schlögl’s first model) on a lattice: Monte Carlo calculations of critical behaviour, Ann. Phys.-new. York. **122**, 373 (1979).
- [38] M. A. Gibson and J. Bruck, Efficient Exact Stochastic Simulation of Chemical Systems with Many Species and Many Channels, J. Phys. Chem. A **104**, 1876 (2000).
- [39] S. Lübeck, Universal scaling behavior of non-equilibrium phase transitions, Int. J. Mod. Phys. B **18**, 3977 (2004).
- [40] In DEP, the exponents Θ and δ are non-universal, as they depend on the initial distributions of the A and B particles [14]. We systematically used Poissonian distribution.
- [41] E. K. Riedel and F. J. Wegner, Effective critical and tricritical exponents, Phys. Rev. B **9**, 294 (1974).
- [42] P. Grassberger, Directed percolation in 2+1 dimensions, J. Phys. A **22**, 3673 (1989).
- [43] H. Hinrichsen, Nonequilibrium Critical Phenomena and Phase Transitions into Absorbing States, Adv. Phys. **49**, 815 (2000).
- [44] M. Dickison and T. Vojta, Monte Carlo simulations of the smeared phase transition in a contact process with extended defects, J. Phys. A **38**, 1199 (2005).
- [45] F. Iglói and C. Monthus, Strong disorder RG approach – a short review of recent developments, Eur. Phys. J. B **91**, 290 (2018).
- [46] J. Hooyberghs, F. Iglói, and C. Vanderzande, Strong Disorder Fixed Point in Absorbing-State Phase Transitions, Phys. Rev. Lett. **90**, 100601 (2003).

- [47] T. Vojta and M. Dickison, Critical behavior and Griffiths effects in the disordered contact process, *Phys. Rev. E* **72**, 036126 (2005).
- [48] T. Vojta, Rare region effects at classical, quantum and nonequilibrium phase transitions, *J. Phys. A* **39**, R143 (2006).
- [49] S. Hladyszau, K. Guan, N. Nivedita, B. Errede, D. Tsygankov, and T. C. Elston, Multiscale Modeling of Bistability in the Yeast Polarity Circuit, *Cells* **13**, 1358 (2024).
- [50] W. M. Śmigiel, L. Mantovanelli, D. S. Linnik, M. Punter, J. Silberberg, L. Xiang, K. Xu, and B. Poolman, Protein diffusion in *Escherichia coli* cytoplasm scales with the mass of the complexes and is location dependent, *Sci. Adv.* **8**, eabo5387 (2022).
- [51] W. Y. C. Huang, X. Cheng, and J. E. Ferrell, Cytoplasmic organization promotes protein diffusion in *Xenopus* extracts, *Nat. Commun.* **13**, 5599 (2022).
- [52] R. M. Garner, A. T. Molines, J. A. Theriot, and F. Chang, Vast heterogeneity in cytoplasmic diffusion rates revealed by nanorheology and Doppelgänger simulations, *Biophys. J.* **122**, 767 (2023).
- [53] I. Muniz, A. Galindo, and M. A. Garcia, Cubic Spline Population Density Functions and Satellite City Delimitation: The Case of Barcelona, *Urban Stud.* **40**, 1303 (2003).
- [54] D. Gu, K. Andreev, and M. E. Dupre, Major Trends in Population Growth Around the World, *China CDC Weekly* **3**, 604 (2021).
- [55] L. M. A. Bettencourt, J. Lobo, D. Helbing, C. Kühnert, and G. B. West, Growth, innovation, scaling, and the pace of life in cities, *Proc. Natl. Acad. Sci.* **104**, 7301 (2007).
- [56] V. Verbavatz and M. Barthelemy, The growth equation of cities, *Nat* **587**, 397 (2020).
- [57] R. Louf and M. Barthelemy, Modeling the Polycentric Transition of Cities, *Phys. Rev. Lett.* **111**, 198702 (2013).